Transactions on Machine Intelligence 2(2) (2019) 120-127

ISSN Online: 2821-1693

Transactions on Machine Intelligence

Journal Homepage: https://tmachineintelligence.ir/index.php/TMI

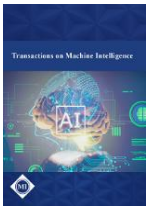

Design of a New Triple-Band Frequency Selective Surface for Filtering WiMAX, WLAN, and X Bands

M. Bashiri[1,*]

[1] Assistant Professor, Department of Electrical Engineering, Faculty of Engineering, Islamic Azad University, Miandoab Branch, Miandoab, Iran

ARTICLE INFO

Article History:
Received 8 March 2019
Received in revised form 20 April 2019
Accepted 18 June 2019
Available online 25 June 2019

Keywords:
Base Unit Cell, Frequency Selective Surface, Triple-Band Filtering

ABSTRACT

This paper proposes a novel single-layer Frequency Selective Surface (FSS) designed on an FR4 substrate with a thickness of 1.6 mm for triple-band filtering applications. The proposed FSS structure consists of unit cells with dimensions of 10×10 mm². The design incorporates a square ring at the top layer, accompanied by two symmetrical rectangular rings at the sides and a vertical rectangular branch placed in the center of the rectangular rings on the bottom layer. The conductive elements are made from a perfect conductor to achieve optimal performance. The structure operates across three distinct frequency bands: 3.2 to 3.81 GHz, 4 to 5.82 GHz, and 8.21 to 12.2 GHz, which correspond to WiMAX, WLAN, and X bands, respectively. This triple-band functionality makes the proposed FSS suitable for applications in modern wireless communication systems. The frequency response of the FSS remains stable across various incidence angles for both Transverse Electric (TE) and Transverse Magnetic (TM) polarizations, confirming the robustness and reliability of the structure. Key advantages of the proposed FSS include its smaller physical dimensions compared to previous designs, the simplicity of its conductive elements, and its alignment with widely used frequency bands. These features collectively enhance the potential of the FSS for integration in compact and efficient filtering systems, offering significant improvements over traditional multi-band filters.

1. INTRODUCTION

With the development of telecommunication networks, which have significantly advanced human communication worldwide, the radiative signals from these devices have caused adverse health effects and destructive impacts on various electronic devices. To minimize these adverse effects, researchers in telecommunications have sought effective solutions, resulting in the design and construction of filters to eliminate or reduce the harmful effects of electromagnetic wave interference. Despite the benefits of these designed filters, drawbacks such as high construction costs and bulky structures have been observed. Thus, telecommunications designers have explored alternatives. The simplicity of structure and lower construction costs, along with the flexible and multifunctional performance of Frequency Selective Surfaces (FSS), make them a suitable replacement for filters.

* Corresponding Author: m.bashiri0441@yahoo.com
Assistant Professor, Department of Electrical Engineering, Faculty of Engineering, Islamic Azad University, Miandoab Branch, Miandoab, Iran

http://dx.doi.org/10.47176/TMI.2019.120

© 2019 by the authors. Licensee T.M.I, Tehran, Iran. This article is an open access article distributed under the terms and conditions of the Creative Commons Attribution (CC-BY) license (http://creativecommons.org/licenses/by/4.0/).

FSS consists of an array of identical elements arranged periodically, exhibiting filtering properties [1]. The identical elements forming these surfaces are referred to as unit cells. The elements in FSS are categorized into four types: first type as N-pole elements, second type as ring elements, third type as planar elements, and fourth type as combinations of the first three types [2]. Previous studies indicate that ring elements, belonging to the second type, demonstrate high efficiency and are often employed in FSS design. This type of element is also utilized in the design of the base unit cell in this paper.

These surfaces are classified into single-layer [3,4,5,6], multi-layer [7,8], and reconfigurable structures [9,10]. To increase the frequency bandwidth in new designs, multi-layer structures can be used, which create more resonances leading to a broader operating bandwidth. Considering economic and technical aspects such as simplicity of structure, cost, and fabrication capabilities, this paper focuses on analyzing and designing a single-layer FSS with simple elements. Previous studies highlight multiple and diverse applications for these FSS surfaces, including satellite applications [11], antennas with beam-steering capabilities [12], absorbers [13,14], radomes [15], electromagnetic shielding [9], and energy consumption optimization [18].

The primary objectives of this paper are summarized as follows:

- Introducing a new single-layer FSS structure

- Designing a base structure with suitable and simple elements to achieve optimal performance and align the operating band with widely used frequency bands

- Ensuring the proposed unit cell elements are simpler and smaller compared to previous designs

- Developing a triple-band design

As seen from the stated objectives, the new base cell design considers all technical and economic factors, fabrication and testing facilities, and associated costs. The proposed unit cell is a single-layer structure on an FR4 substrate with a thickness of 1.6 mm, a dielectric constant of 4.4, and a loss tangent of 0.02. The unit cell dimensions are 10×10 mm². On the bottom side of the substrate, a square ring element with two symmetrical rectangular rings on the sides and two vertical rectangular branches in the middle of the rectangular rings is placed, while only a square ring is located on the top side. By adjusting the dimensions and positions, the operating frequency band ranges from 5.41 to 11.01 GHz, covering substantial portions of the X and WLAN bands. A stable frequency response is achieved for various incidence angles in both TE and TM polarizations, demonstrating the proposed structure's reliable performance.

2. ANALYSIS AND DESIGN OF BASE UNIT CELL

Figure 1 shows the proposed unit cell, with dimensions of 10×10 mm², printed on an FR4 substrate with a thickness of 1.6 mm, a dielectric constant of 4.4, and a loss tangent of 0.02. On the bottom side of the substrate, two rectangular ring elements with a thickness of 0.5 mm and two vertical rectangular branches with a length of 3 mm and a width of 0.5 mm are placed. A square ring element with a thickness of 0.3 mm is printed on the top side.

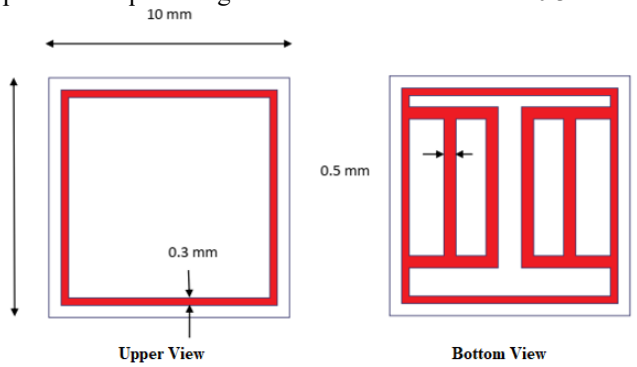

Fig. 1. Proposed base unit cell design.

The exact dimensions of these elements are specified in Figure 1. The frequency behavior of this designed FSS structure is analyzed step by step. In the first step, only one square ring is placed on one side of the cell. In the second step, another square ring is added to the bottom side. Two symmetrical rectangular rings are added to the sides of the square ring on the bottom side in the third step. Finally, in the fourth step, two vertical rectangular branches are added in the middle of the rectangular rings on the bottom side.

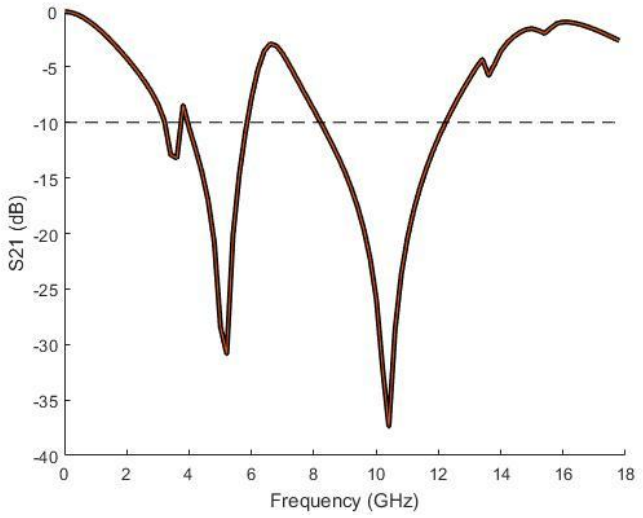

Fig. 2. S21 curve of the FSS unit cell.

In the S21 curve, frequencies below the -10 dB line are part of the stopband, while other frequencies belong to the passband. The results in Figure 2 show resonances at 3.41 GHz, 5.21 GHz, and 10.41 GHz. The frequency bandwidth ranges from 3.20 to 3.81 GHz, 4 to 5.82 GHz, and 8.21 to 12.2 GHz, covering substantial portions of the WiMAX, WLAN, and X bands.

3. SURFACE CURRENT DISTRIBUTION ANALYSIS

For a more detailed analysis of the FSS's performance, the surface current distribution is studied. Figure 3 shows the surface current distribution at the resonant frequencies of 3.41 GHz, 5.21 GHz, and 10.41 GHz. Red and dark blue in the color bar represent strong and weak current distributions on the FSS unit cell, respectively. From the charts in Figure 4, it is observed that at 3.41 GHz, the current flows on the square rings on the top and bottom sides and part of the rectangular elements on the bottom side. At 5.21 GHz and 10.41 GHz, a larger portion of the elements on the top side and part of the conductive elements on the bottom side are radiated.

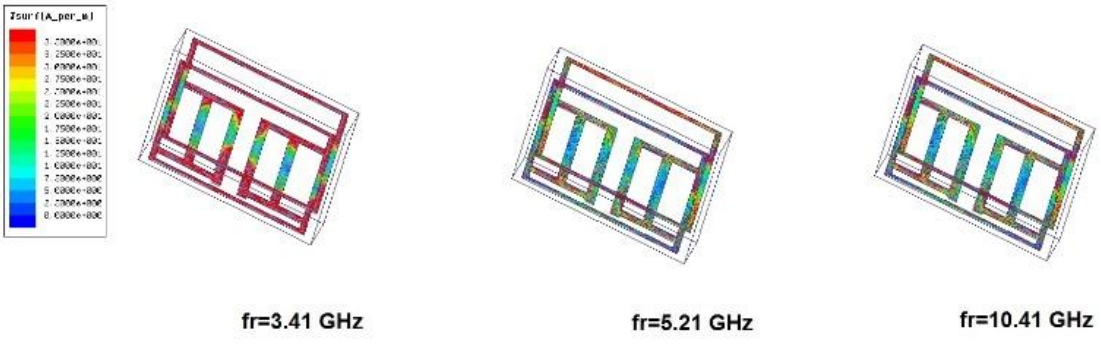

Fig. 3. Surface current distribution charts at three resonant frequencies.

As observed in the unit cell design stages, the square rings on the top and bottom sides and part of the elements on the bottom side are responsible for these resonances. The square rings on the top and bottom sides trigger the 3.41 GHz resonance frequency.

4. FREQUENCY RESPONSE STABILITY ANALYSIS AGAINST ANGLE AND POLARIZATION VARIATIONS

Considering that various waves with different incidence angles and polarizations hit an FSS surface, a sensitivity analysis is conducted to evaluate the stable frequency response against angle and polarization variations.

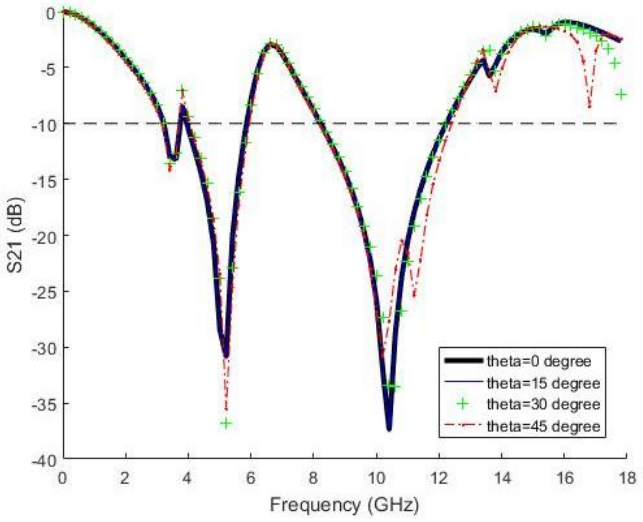

Fig. 4. S21 curves for different incidence angles in TE polarization.

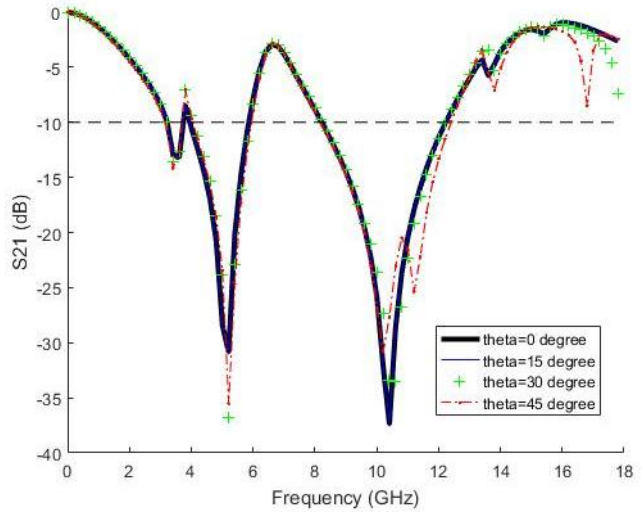

Fig. 5. S21 curves for different incidence angles in TM polarization.

The proposed structure's performance is analyzed for different incidence angles in both TM and TE polarizations. From Figures 4 and 5, it is observed that a stable response is achieved for various incidence angles in both TM and TE polarizations. Incidence angles are analyzed from 0 to 45 degrees with a 15-degree step. Although a slight variation is observed at the 45-degree angle for the 10.41 GHz resonance frequency, the stopband remains unaffected, stable, and consistent. The frequency response demonstrates the proposed design's acceptable performance.

5. PARAMETRIC ANALYSIS OF THE UNIT CELL

To evaluate the effect of element dimensions on the frequency response, a parametric analysis of this structure is conducted. The width of the vertical rectangular branches on the bottom side is one of the critical parameters influencing the frequency response of the base unit cell. As shown in Figure 6, Y denotes the width of the vertical

rectangular branch, which is 0.5 mm. The analysis is conducted for four different Y values. As observed from the results in Figure 6, no change is seen for Y values of 0.3 mm.

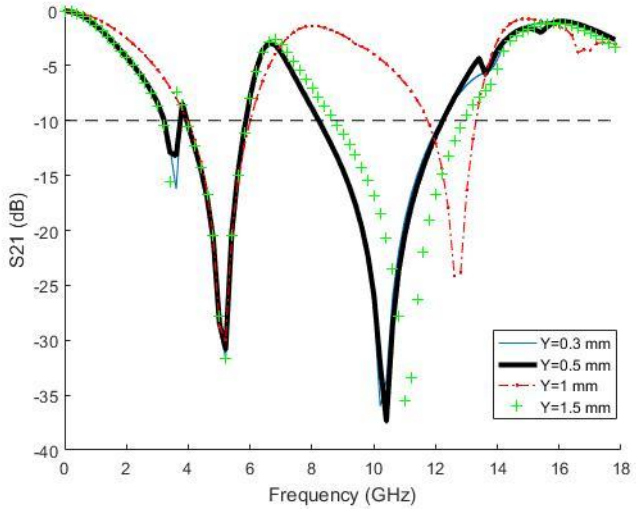

Fig. 6. S21 curves for four different Y values.

However, for values of 1 and 1.5 mm, the resonance frequency of the third band increased, and for 1 mm, the third band bandwidth decreased. As observed from the curves, the best results were obtained for Y values of 0.3 and 0.5 mm. To investigate the role of the substrate on FSS performance, a parametric analysis was conducted with different substrates. The analysis was performed with three different substrates: RT Duriod 5880C with a relative dielectric constant of 2.2, FR4 with a relative dielectric constant of 4.4, and RT Duriod RO6006 with a relative dielectric constant of 15.6. The results, compared in Figure 7, clearly indicate that as the dielectric constant increases, the operational bandwidth decreases. This behavior is due to the principle that resonance is inversely proportional to the square root of the dielectric constant. For RT Duriod 5880C with a dielectric constant of 2.2, the operational bandwidth ranges from 4.2 to 4.61 GHz, 5.41 to 7.41 GHz, and 11.41 to 15.61 GHz. For FR4 with a dielectric constant of 4.4, it ranges from 3.2 to 3.81 GHz, 4 to 5.82 GHz, and 8.21 to 12.2 GHz. For RT Duriod RO6006 with a dielectric constant of 15.6, it ranges from 2.61 to 3.21 GHz, 3.41 to 5.21 GHz, and 7.01 to 10.61 GHz.

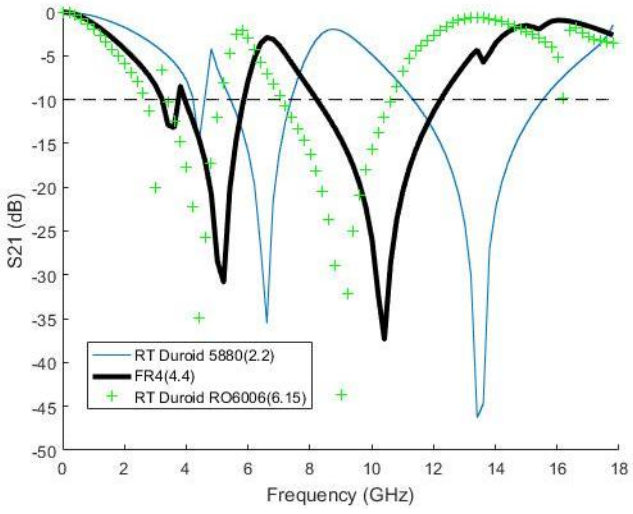

Fig. 7. S21 curves for three different dielectric constant values.

6. CONCLUSION

This paper presents a single-layer design with simple elements, demonstrating that the proposed structure's dimensions are smaller and its operational bandwidth is acceptable compared to previous designs. The stopband frequency range spans from 3.2 to 3.81 GHz, 4 to 5.82 GHz, and 8.21 to 12.2 GHz, covering the widely used WLAN, WiMAX, and X bands. The proposed single-layer FSS has a simple structure and low manufacturing cost. The designed FSS consists of an FR4 substrate with a thickness of 1.6 mm, with conductive elements on both sides of the substrate. A square ring is located on the bottom side, and two rectangular rings with a rectangular branch in the middle of the rings are symmetrically placed on the bottom side. Only a simple square ring is placed on the top side. By accurately selecting the dimensions and positions of the conductive elements, three frequency bands are achieved, covering the WLAN, WiMAX, and X bands.

The proposed FSS exhibits a stable frequency response against incidence angle variations for both TM and TE polarizations. The new design is triple-banded with desirable operational bandwidth and is smaller and simpler than previously constructed similar designs, making it a suitable choice for filtering applications in telecommunication systems.

Transparency Statement

The data supporting this study are available upon reasonable request to the corresponding author, subject to ethical and confidentiality considerations.

Acknowledgments

We would like to express our gratitude to all individuals who contributed to this project.

Declaration of Interest

The authors declare that they have no competing interests.

Funding

This research received no specific grant from any funding agency, commercial, or not-for-profit sectors.

REFERENCES

[1] Munk, B. A. (2000). Frequency Selective Surfaces: Theory and Design (1st ed.). Wiley-Interscience. https://doi.org/10.1002/0471723770

[2] Bharti, G., Jha, K. R., & Singh, G. (2014). A synthesis technique of single square loop frequency selective surface at terahertz frequency. Optik, 125(21), 6428-6435. https://doi.org/10.1016/j.ijleo.2014.08.009

[3] Nauman, M., Saleem, R., Rashid, A. K., & Shafique, M. F. (2016). A miniaturized flexible frequency selective surface for X-band applications. https://doi.org/10.1109/TEMC.2015.2508503

[4] Ferreira, D., Cuiñas, I., Caldeirinha, R. F., & Fernandes, T. R. (2016). Dual-band single-layer quarter ring frequency selective surface for Wi-Fi applications. IET Microwaves, Antennas & Propagation, 10(4), 435-441. https://doi.org/10.1049/iet-map.2015.0641

[5] Bashiri, M., Ghobadi, C., Nourinia, J., & Majidzadeh, M. (2018). An explicit single-layer frequency selective surface design with wide stop band frequency response. International Journal of Microwave and Wireless Technologies, 10(7), 819-825. https://doi.org/10.1017/S1759078718000260

[6] Bashiri, M., Ghobadi, C., Nourinia, J., & Majidzadeh, M. (2017). WiMAX, WLAN, and X-band filtering

mechanism: Simple-structured triple-band frequency selective surface. IEEE Antennas and Wireless Propagation Letters, 16, 3245-3248. https://doi.org/10.1109/LAWP.2017.2771265

[7] Ghosh, S., Bhattacharyya, S., & Srivastava, K. V. (2016). Design, characterisation and fabrication of a broadband polarisation-insensitive multi-layer circuit analogue absorber. IET Microwaves, Antennas & Propagation, 10(8), 850-855. https://doi.org/10.1049/iet-map.2015.0653

[8] Xu, G., Hum, S. V., & Eleftheriades, G. V. (2018). A technique for designing multilayer multistopband frequency selective surfaces. IEEE Transactions on Antennas and Propagation, 66(2), 780-789. https://doi.org/10.1109/TAP.2017.2772089

[9] Majidzadeh, M., Ghobadi, C., & Nourinia, J. (2016). Novel single layer reconfigurable frequency selective surface with UWB and multi-band modes of operation. AEU - International Journal of Electronics and Communications, 70(2), 151-161. https://doi.org/10.1016/j.aeue.2015.10.011

[10] Ebrahimi, A., Shen, Z., Withayachumnankul, W., Al-Sarawi, S. F., & Abbott, D. (2016). Varactor-tunable second-order bandpass frequency-selective surface with embedded bias network. IEEE Transactions on Antennas and Propagation, 64(5), 1672-1680. https://doi.org/10.1109/TAP.2016.2537378

[11] Sheng, X., Ge, J., Han, K., & Zhu, X. C. (2018). Transmissive/reflective frequency selective surface for satellite applications. IEEE Antennas and Wireless Propagation Letters, 17(7), 1136-1140. https://doi.org/10.1109/LAWP.2018.2830408

[12] Han, L., Cheng, G., Han, G., Ma, R., & Zhang, W. (2019). Electronically beam-steering antenna with active frequency-selective surface. IEEE Antennas and Wireless Propagation Letters, 18(1), 108-112. https://doi.org/10.1109/LAWP.2018.2882525

[13] Bakir, M., Delihacioglu, K., Karaaslan, M., Dincer, F., & Sabah, C. (2016). U-shaped frequency selective surfaces for single- and dual-band applications together with absorber and sensor configurations. IET Microwaves, Antennas & Propagation, 10(3), 293-300. https://doi.org/10.1049/iet-map.2015.0341

[14] Zhang, K., Jiang, W., & Gong, S. (2017). Design bandpass frequency selective surface absorber using LC resonators. IEEE Antennas and Wireless Propagation Letters, 16, 2586-2589. https://doi.org/10.1109/LAWP.2017.2734918

[15] Zhu, H., Huang, J. J., Yuan, N. C., & Yi, B. (2017). Tunable frequency selective radome with broadband absorbing properties. In 2017 Progress in Electromagnetics Research Symposium - Spring (PIERS) (pp. 2922-2926). IEEE. https://doi.org/10.1109/PIERS.2017.8262168

[16] Moubarek, B., Moufida, A., Gharsallah, A., & Nedil, M. (2018). A flexible frequency selective surface for beam-switching applications. In 2018 IEEE International Symposium on Antennas and Propagation & USNC/URSI National Radio Science Meeting (pp. 2023-2024). IEEE. https://doi.org/10.1109/apusncursinrsm.2018.8608783

[17] Chen, H., Lu, W. B., Liu, Z. G., Zhang, J., Zhang, A. Q., & Wu, B. (2018). Experimental demonstration of microwave absorber using large-area multilayer graphene-based frequency selective surface. IEEE Transactions on Microwave Theory and Techniques, 66(8), 3807-3816. https://doi.org/10.1109/TMTT.2018.2834510

[18] Majidzadeh, M. (2019). A proposed modified energy-reducing glass structure for energy management of HVAC systems and improvement of communication bands. Journal of Energy Engineering and Management, 9(1), 48-55.